

Réduction de modèle

Application aux écoulements décollés

Bérénice Podvin
EM2C, CentraleSupélec, Université Paris-Saclay

Journée SFT: Apport des modèles réduits dans la modélisation des transferts thermiques

Context

Machine Learning

Digital Twin

Complex physics

Representation

Model order reduction

High-dimensional observations

**Physics-informed/
guided/aware models**

Data Science

Data assimilation

POD reduced-order models

1. Data-driven representation: empirical Karhunen-Loève basis
2. Physics-based model: Galerkin projection + closure
3. Application to separated flows
4. Summary

The Karhunen-Loève theorem

- Let $u(\eta)$ be a centered stochastic process defined in $L^2(\Omega)$: $E[u] = 0$
- η is a deterministic variable in a closed bounded set Ω (compact set)
- Let us define the covariance function $K(\eta, \eta') = E[u(\eta)u(\eta')]$
- Mercer theorem: There is a denumerable set of eigenvalues $\lambda_n \geq 0$ and a set of eigenvectors $e_n(\eta)$ such that

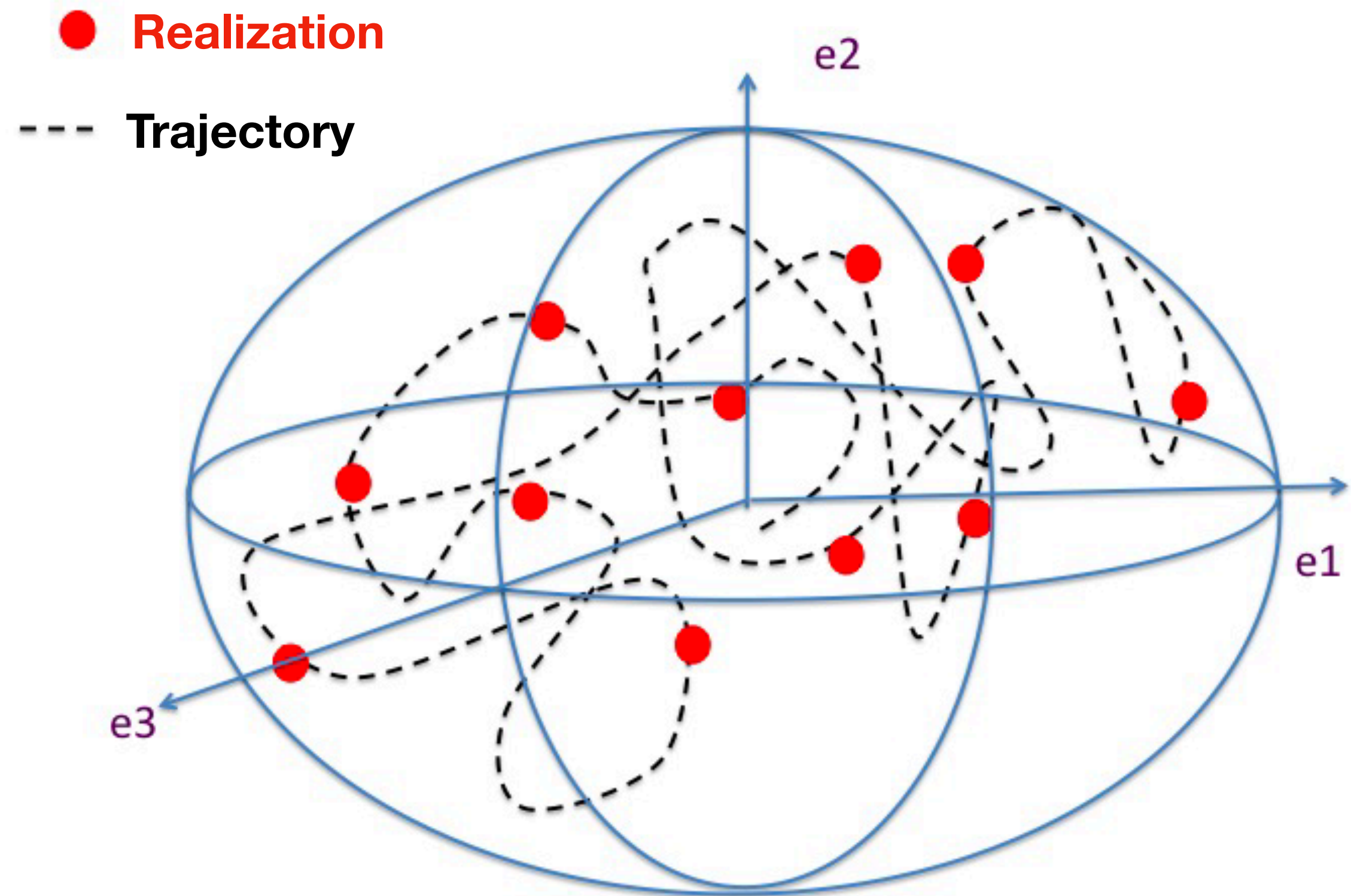
$$K(\eta, \eta') = \sum_{n=1}^{\infty} \lambda_n e_n(\eta) e_n(\eta')$$

Computing the covariance

- Usual choice for a spatio-temporal field (classical POD):
 - Deterministic variables: physical space
 - Stochastic variables: time
- Relies on **ergodicity assumption**: computing the sampled covariance along one trajectory provides a good estimate of the covariance

$$K(\eta, \eta') = \lim_{N \rightarrow \infty} \frac{1}{N} \sum_{n=1}^N u(\eta, t_n) u(\eta', t_n)$$

Interpretation of the empirical modes

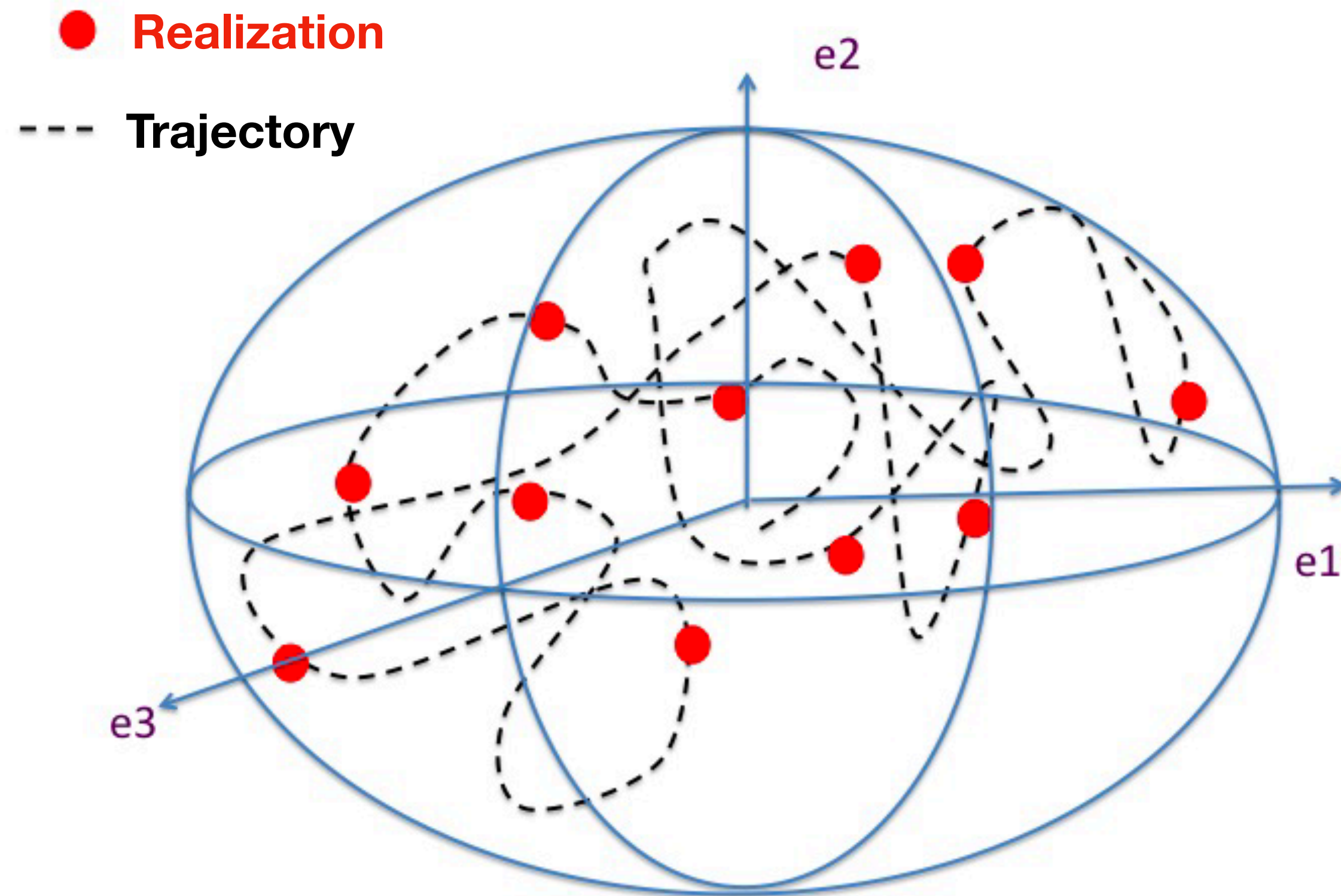


The POD modes are the principal axes of the ellipsoid containing the realizations

⇒ POD of sampled covariance = PCA

PCA: Principal Component Analysis

Interpretation of the empirical modes

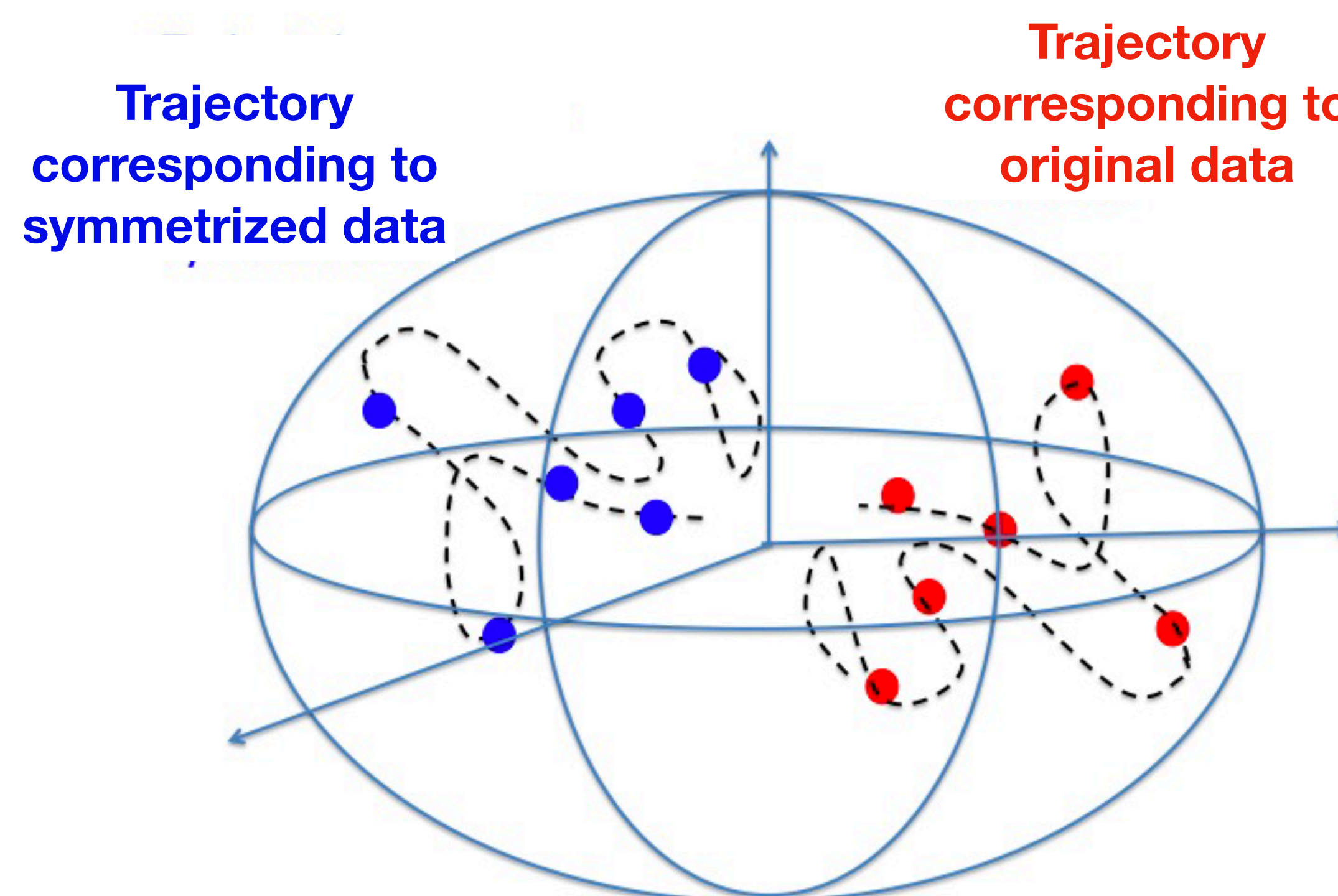


The POD modes are the principal axes of the ellipsoid containing the realizations

⇒ POD of sampled covariance = PCA

PCA: Principal Component Analysis

Should symmetry be enforced in the dataset?



Are we interested in:

- A single trajectory?
- All possible trajectories (lack of ergodicity)?

POD modes are not coherent structures

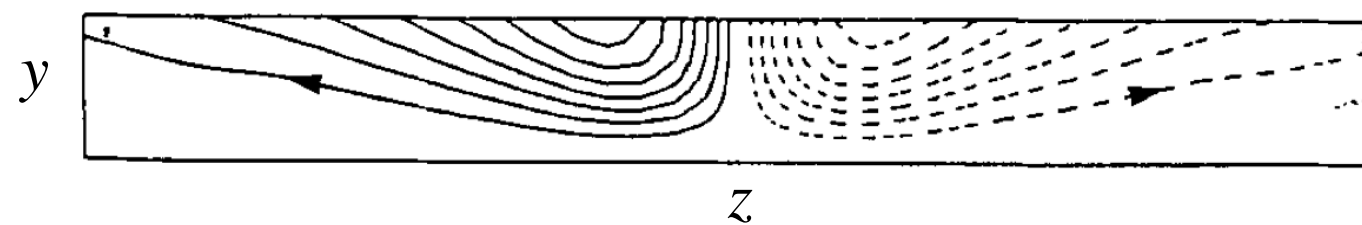
Coherent structures are **localized** in space and time.

POD modes have a **global** support and **integrate** statistical symmetries of the flow.

→ POD modes do not generally coincide with coherent structures which can make physical interpretation difficult.

- Example: Cross-section of the turbulent wall layer

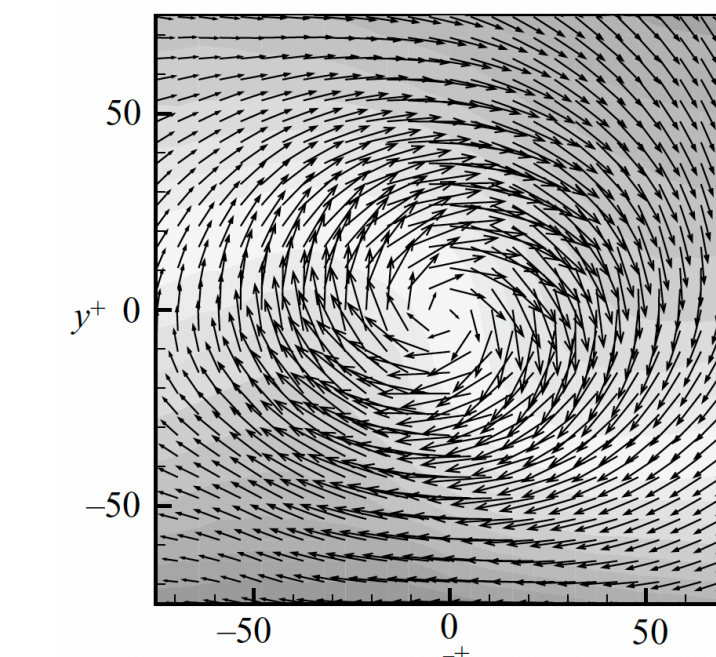
Dominant POD mode (Moin et al. 84)



Symmetric

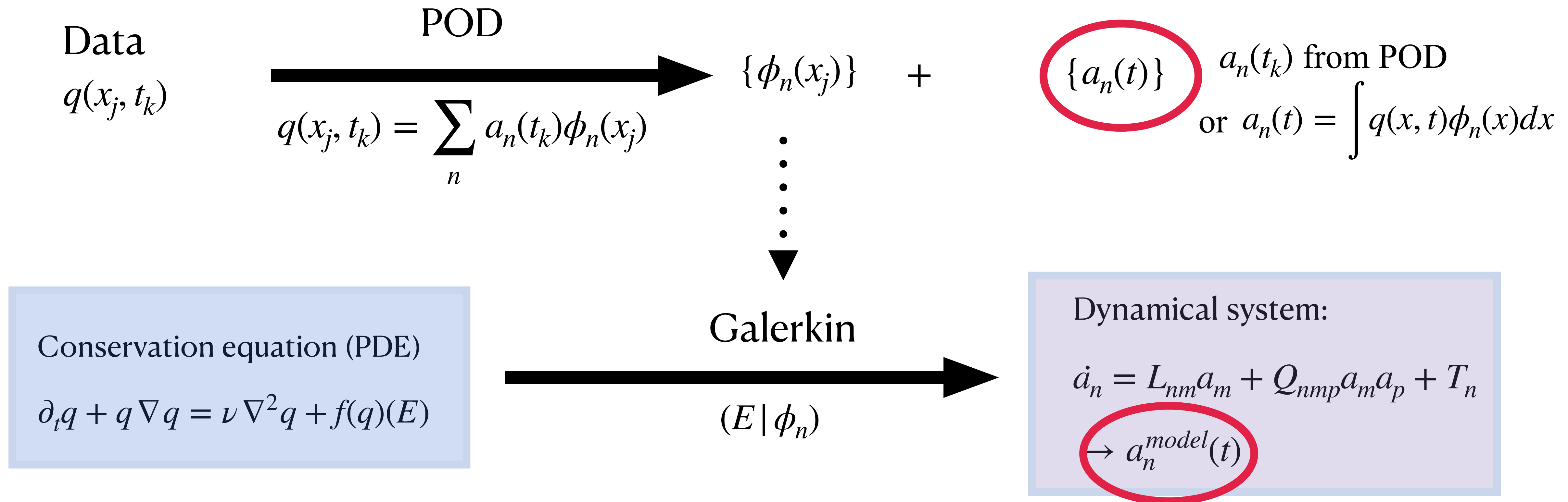
Invariance by spanwise reflection

Conditional eddy structure (Carlier et al. 05)



Asymmetric

Building a low-dimensional model



Application to the incompressible Navier-Stokes equations

1 - Decompose velocity field $\tilde{u} = U + u$ with $U = \bar{u}$

2- Write conservation equations:

$$\frac{\partial u}{\partial t} + U \cdot \nabla u + u \cdot \nabla U + u \cdot \nabla u = -\frac{1}{\rho} \nabla p + \nu \nabla^2 u \quad (E)$$

+ Boundary conditions

3- Apply POD to fluctuating velocity field u and obtain basis $\{\phi_n\}$

4- Mass conservation is naturally enforced by construction $\forall n, \nabla \cdot \phi_n = 0$ (linear property)

5- Introduce expansion $u(x, t) = \sum_{n=1}^N a_n(t) \phi_n(x)$ and project (E) onto mode ϕ_k

Linear terms

$$\bullet \int \frac{\partial u}{\partial t} \cdot \phi_p(x) dx = \sum_{n=1}^N \dot{a}_n(t) \int \phi_n(x) \phi_p(x) dx = \sum_{n=1}^N \dot{a}_n(t) \delta_{np} = \dot{a}_p$$

$$\bullet \int \nabla^2 u \cdot \phi_p(x) dx = \sum_{n=1}^N a_n(t) \int \nabla^2 \phi_n(x) \phi_p(x) dx = \sum_{n=1}^N L_{np}^D a_n(t) \quad L^D \sim \text{diagonal with entries } < 0$$

$$\bullet \int (U \cdot \nabla u + u \cdot \nabla U) \cdot \phi_p(x) dx = \sum_{n=1}^N a_n(t) \int (U \cdot \nabla \phi_n(x) + \phi_n(x) \cdot \nabla U) \cdot \phi_p(x) dx = \sum_{n=1}^N L_{np}^M a_n(t)$$

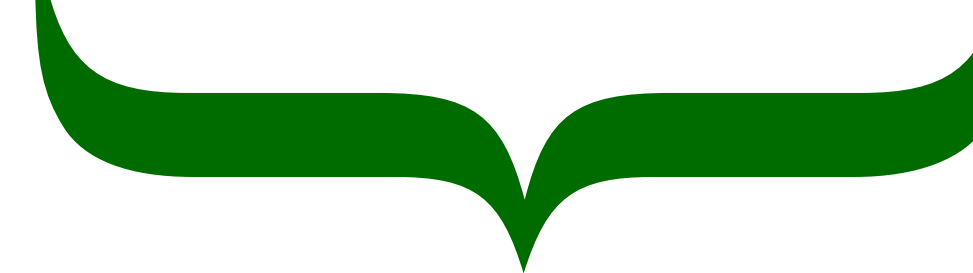
$L^M \sim \geq 0$ large scales extract energy from mean shear

The Reynolds stress tensor

$$\bullet \tau_{ij} = u_i u_j = u_{i,<} u_{j,<} + u_{i,>} u_{j,<} + u_{i,<} u_{j,>} + u_{i,>} u_{j,>}$$



RESOLVED



CROSS-TERMS

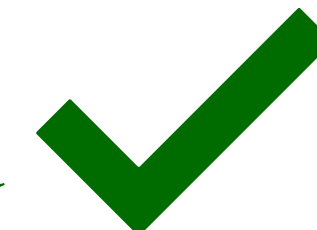


UNRESOLVED

- $u_{i,<} u_{j,<}$: computed with Galerkin procedure (quadratic terms)



- $u_{i,<} u_{j,>} + u_{i,>} u_{j,<}$: Leonard stresses can be neglected



- $u_{i,>} u_{j,>}$: modelled with eddy viscosity hypothesis $\tau_> = 2\mu_T s_<$ with $s_< = \frac{1}{2} (\nabla u_< + \nabla u_<^T)$

The eddy viscosity hypothesis

Heisenberg 1948 « The way in which smaller eddies transfer momentum is similar to ordinary friction »

$$\implies \nabla \cdot \tau_> = \nu_T \nabla^2 u_< \text{ with } \nu_T \propto u_C l_C$$

Aubry et al. 1988

$$\nu_T = \nu_0$$

$$\text{Extra terms } L_{np}^\nu a_n$$

$$L_{np}^\nu = \alpha L_{np}^D$$

Rempfer and Fasel 1994

$$\nu_T = \nu_T(p)$$

$$\text{Extra terms } L_{np}^\nu a_n$$

$$L_{np}^\nu = \alpha_p L_{np}^D$$

Osth et al. 2014

$$\nu_T \propto k_<^{1/2}$$

$$\text{Extra terms } D_p^\nu \left(\sum_n |a_n|^2 \right)^{1/2} a_p$$

$$k_< = \sum_{n=1}^N |a_n|^2$$

Podvin and Sergent 2017

$$\nu_T \propto k_<^{1/2} \approx \bar{k}_<^{1/2} \left(1 + \frac{1}{2} \frac{k'_<}{\bar{k}_<} \right) = \frac{1}{2} \bar{k}_<^{1/2} \left(1 + \frac{k'_<}{\bar{k}_<} \right)$$

$$\text{Extra terms } C_{pn} \sum_{m=1}^N (\lambda_m + |a_m|^2) a_n$$

- ν_T bifurcation parameter for model
- Extra information needed to determine ν_T (e.g. DNS)

The effect of unresolved scales

- Coherent part with cubic term and linear term L^ν . If L^ν has the same structure as L^D :

$$L^D \text{ nearly diagonal and negative} \implies L_{np}^\nu = \delta_{np} L_{pp}^\nu = -\alpha_p \delta_{np} \sum \lambda_i, C_{np} = -\alpha_p \delta_{np}$$

- Incoherent part modelled by noise ϵ_p

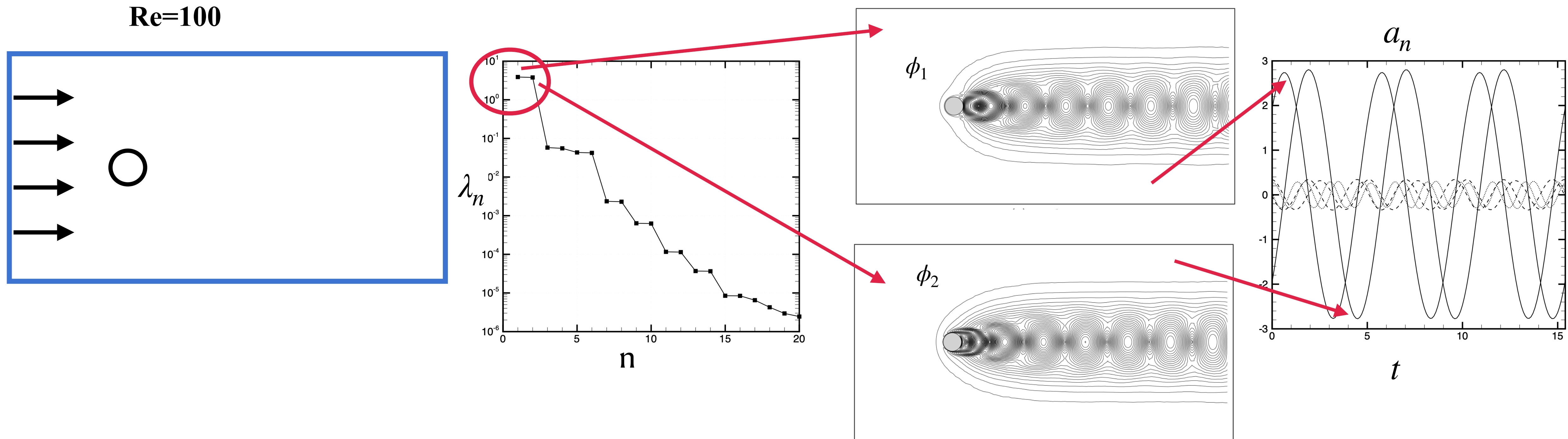
\implies Final form of the model:

$$\dot{a}_p = L_{np} a_n + Q_{nmp} a_n a_m - \alpha_p a_i^2 a_p + \epsilon_p \text{ with } L = L^D + L^M + L^\nu$$

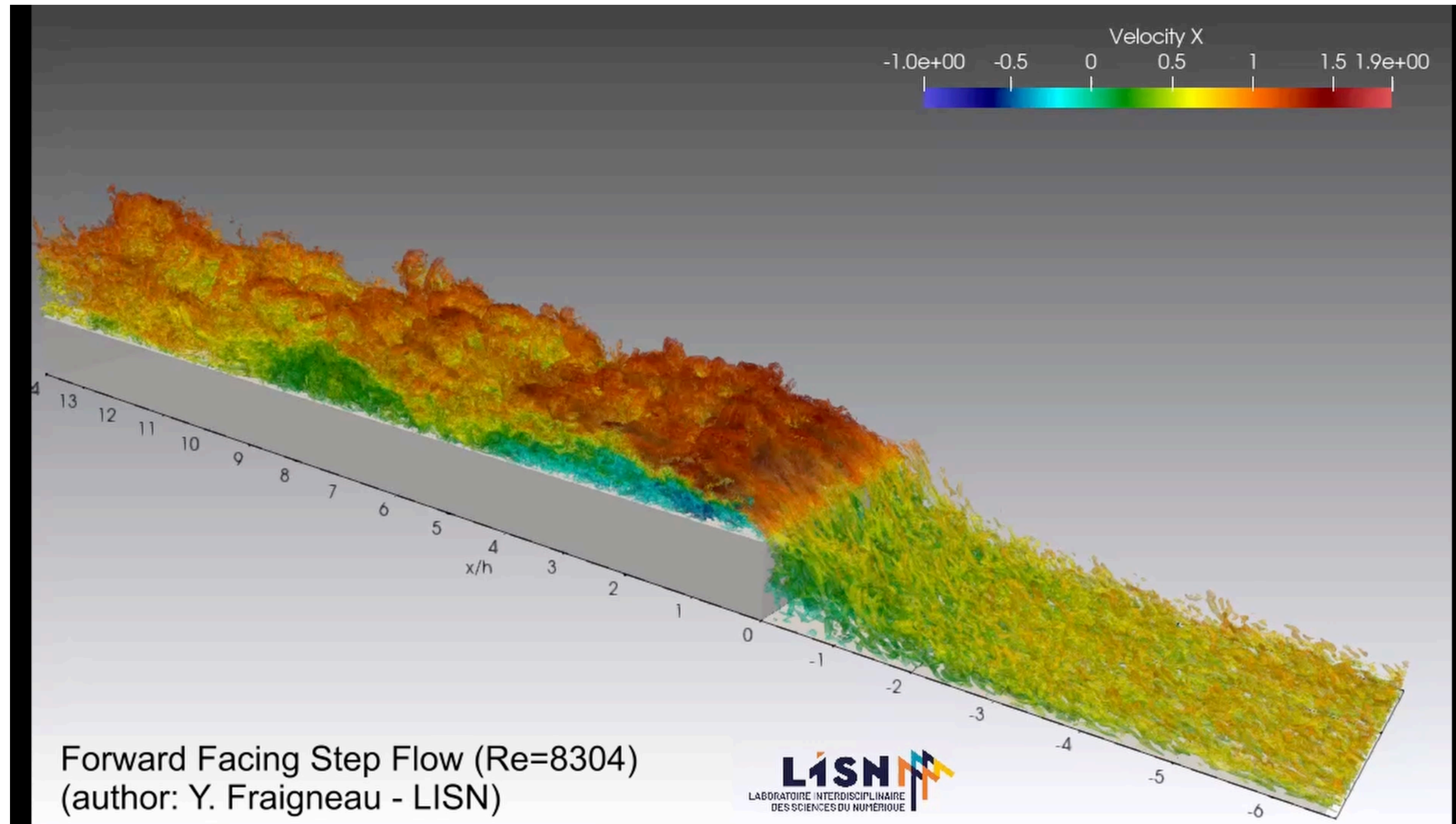
where α_p is determined from observations of $a_n(t)$

A first example: cylinder flow

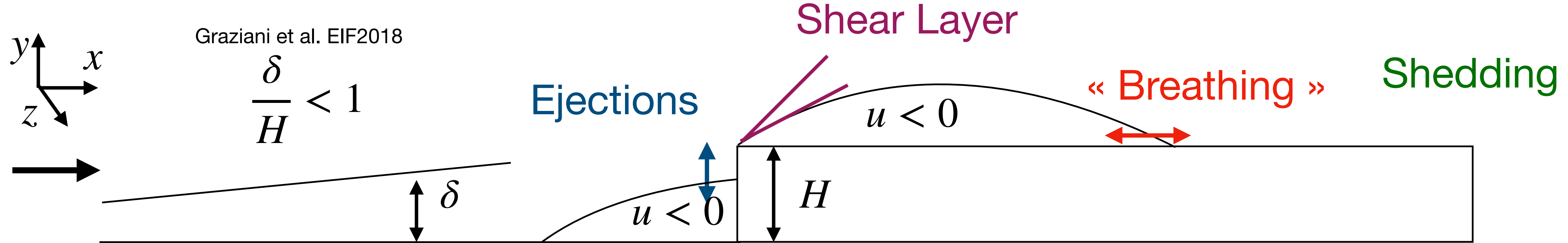
2-D flow behind a cylinder (Cordier and Bergmann 06)



A second example: the forward-facing step



The key dynamics

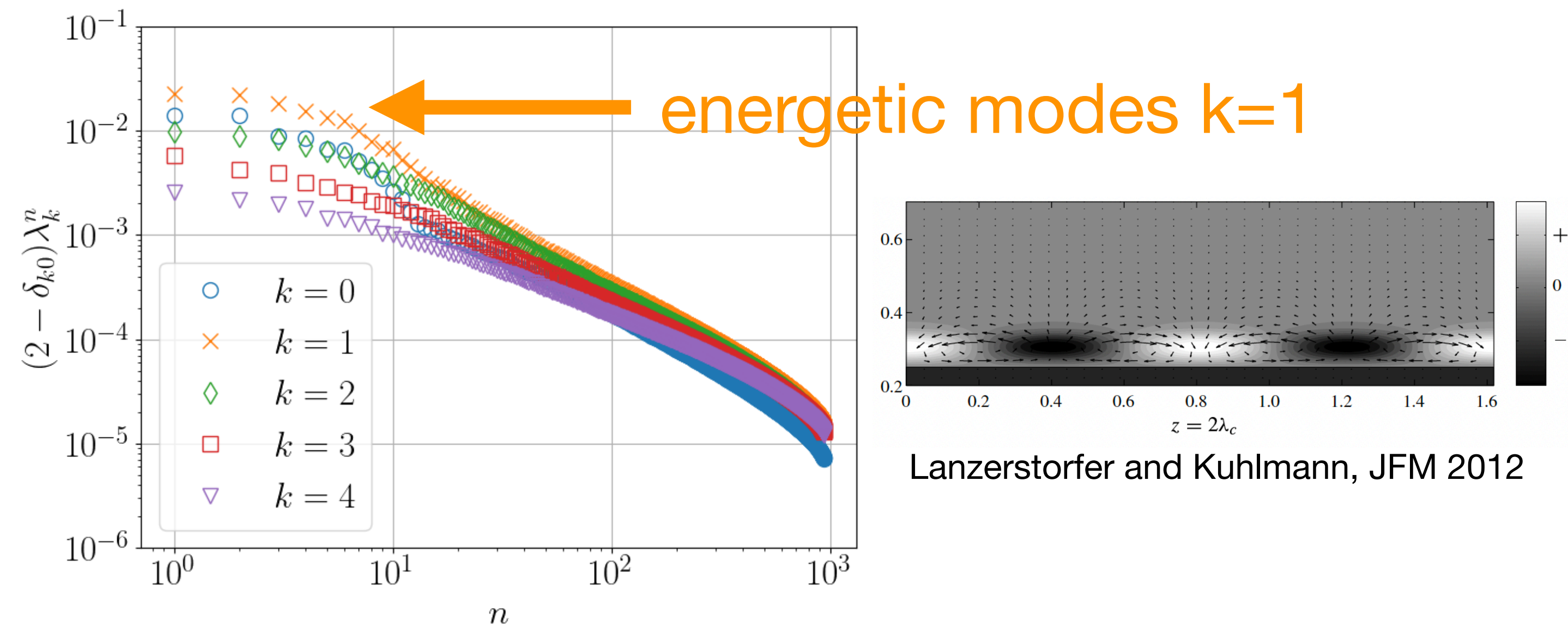


Collab PPRIME (F. Kerhervé), U. Calgary (E. Larose, R. Martinuzzi)

Homogeneity in spanwise direction

→ Fourier representation in z:

$$u(x, y, z, t) = \sum_k \sum_n a_k^n(t) \phi_k^n(x, y) e^{2i\pi z/L_z}$$



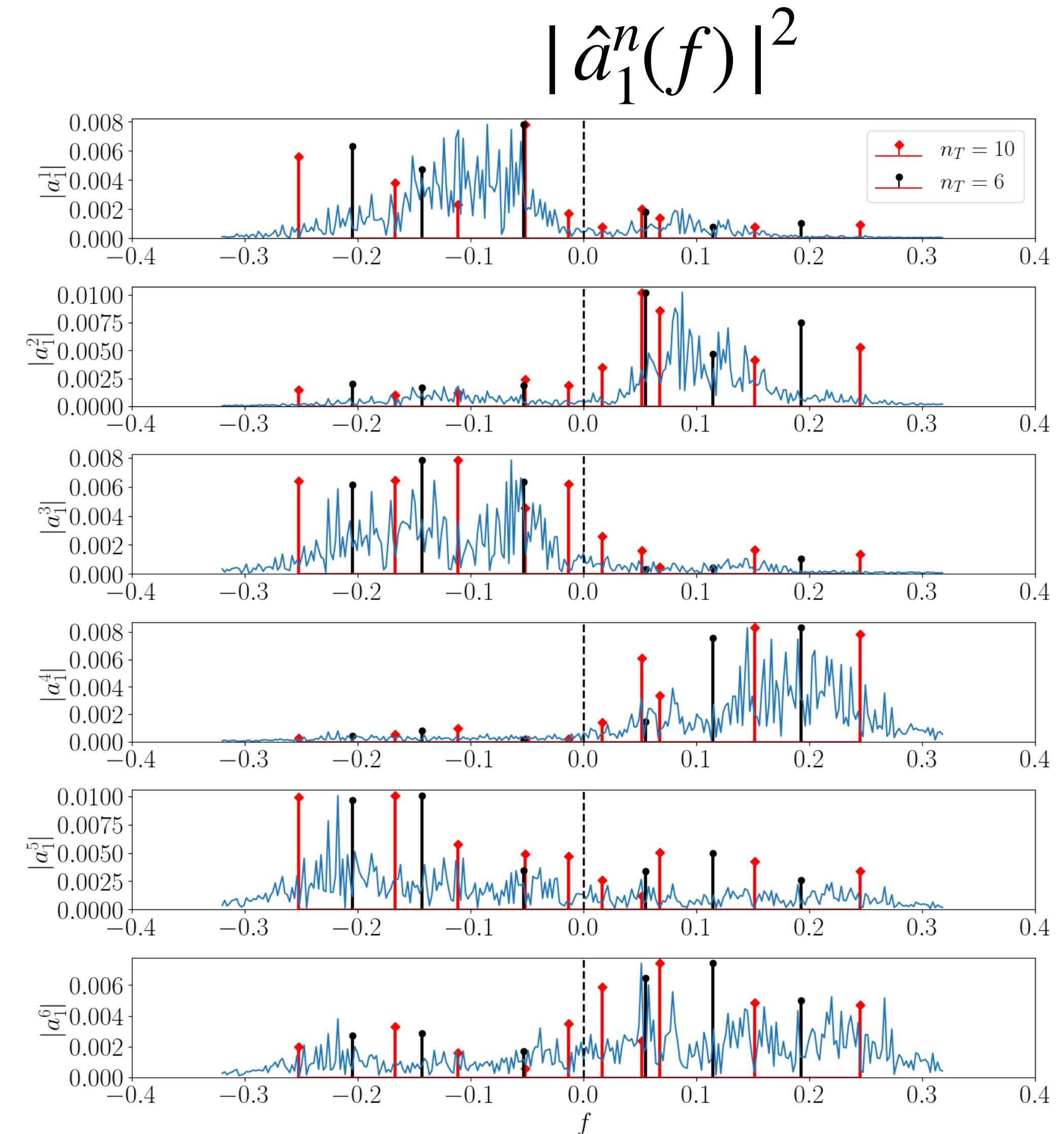
A basic model

Model with constant mean flow
(does not account for ejections)

$$\rightarrow \dot{a}_k^n = L_{nm} a_k^m$$

Results robust w.r.t $n_T \geq 6$

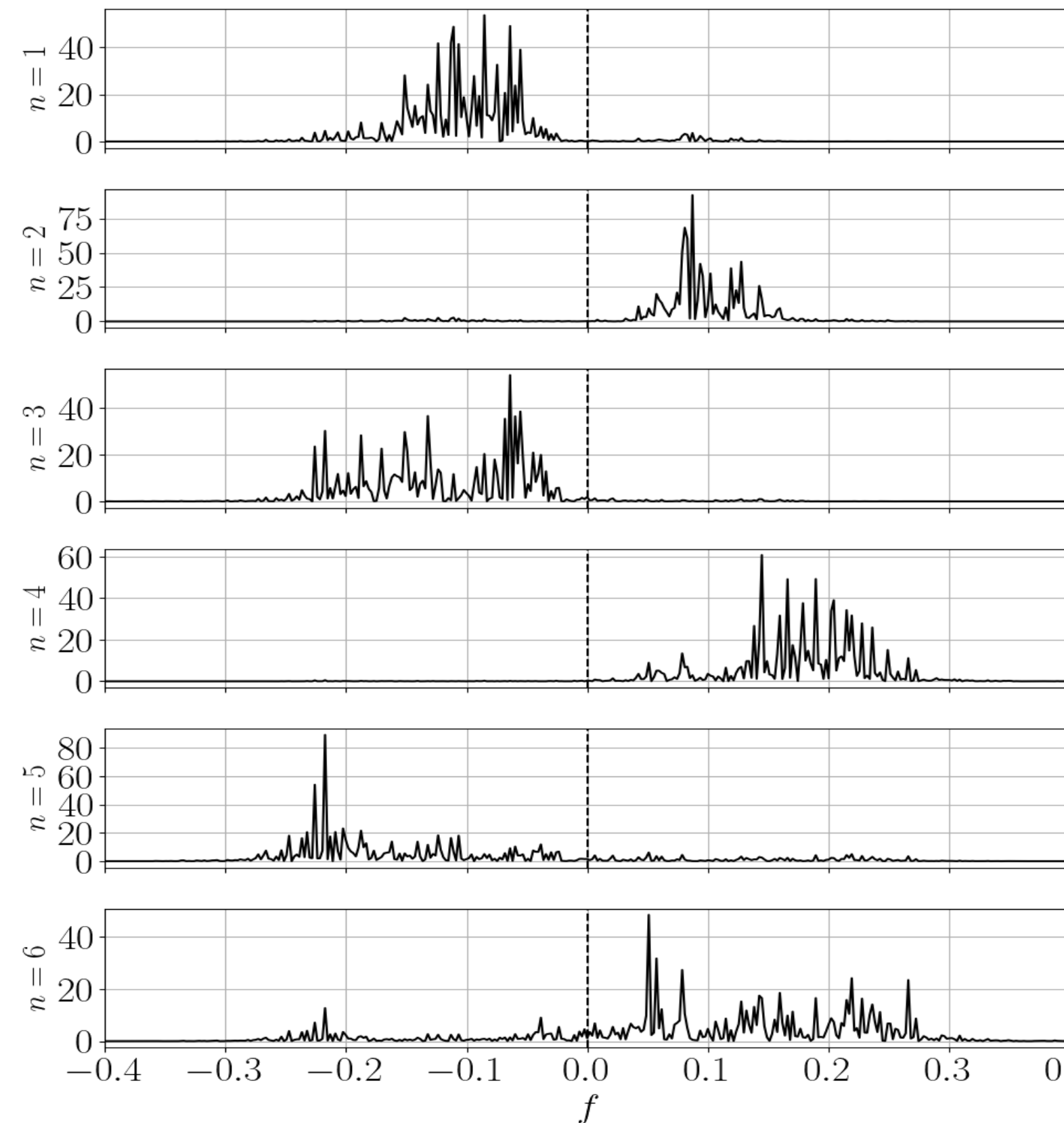
Discrete frequencies match DNS
frequency spectrum



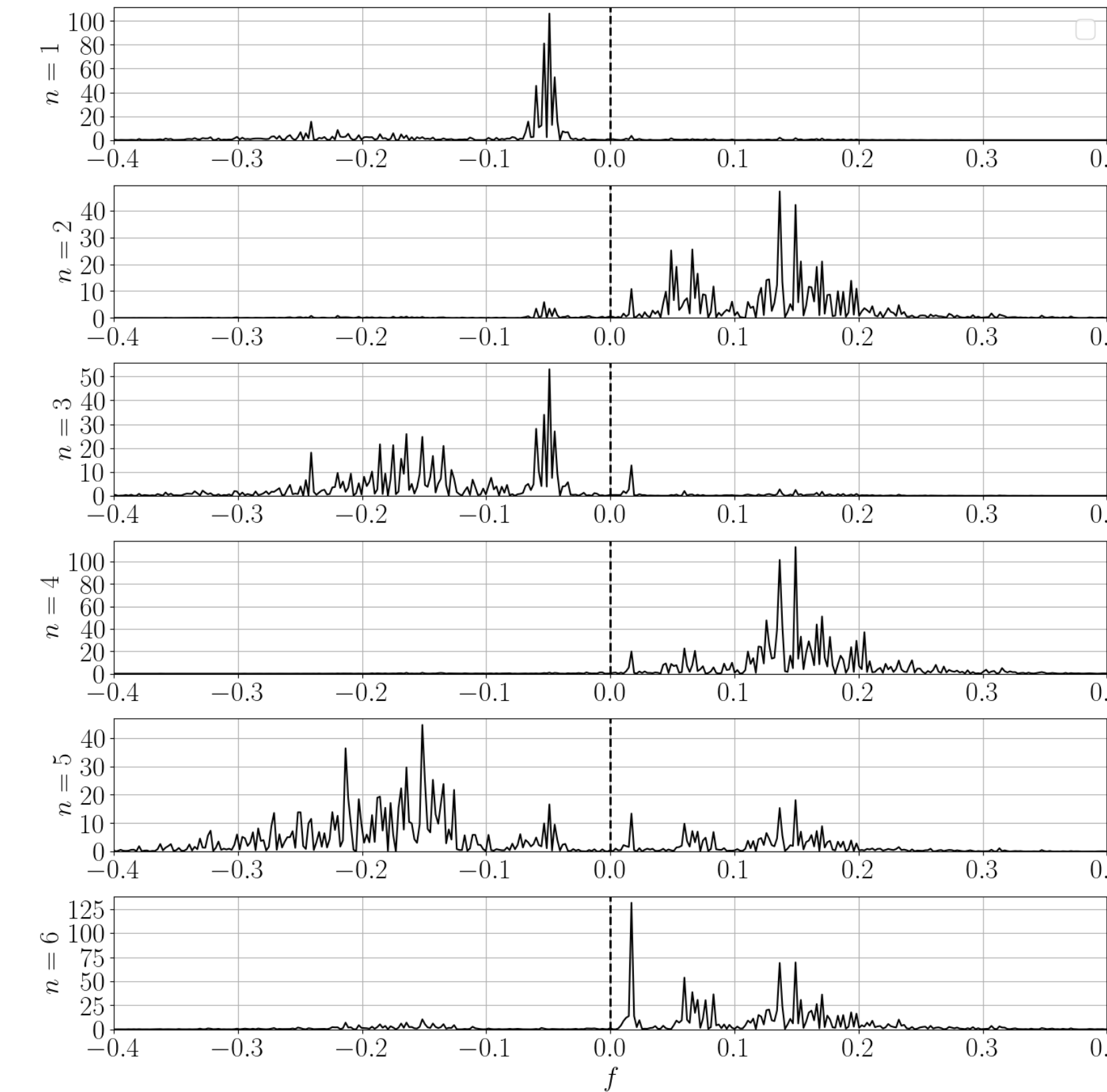
A (slightly less) basic model

→ $\dot{a}_k^n = \tilde{L}_{nm}(t)a_k^m$ where \tilde{L} varies like the maximum shear at the edge

DNS

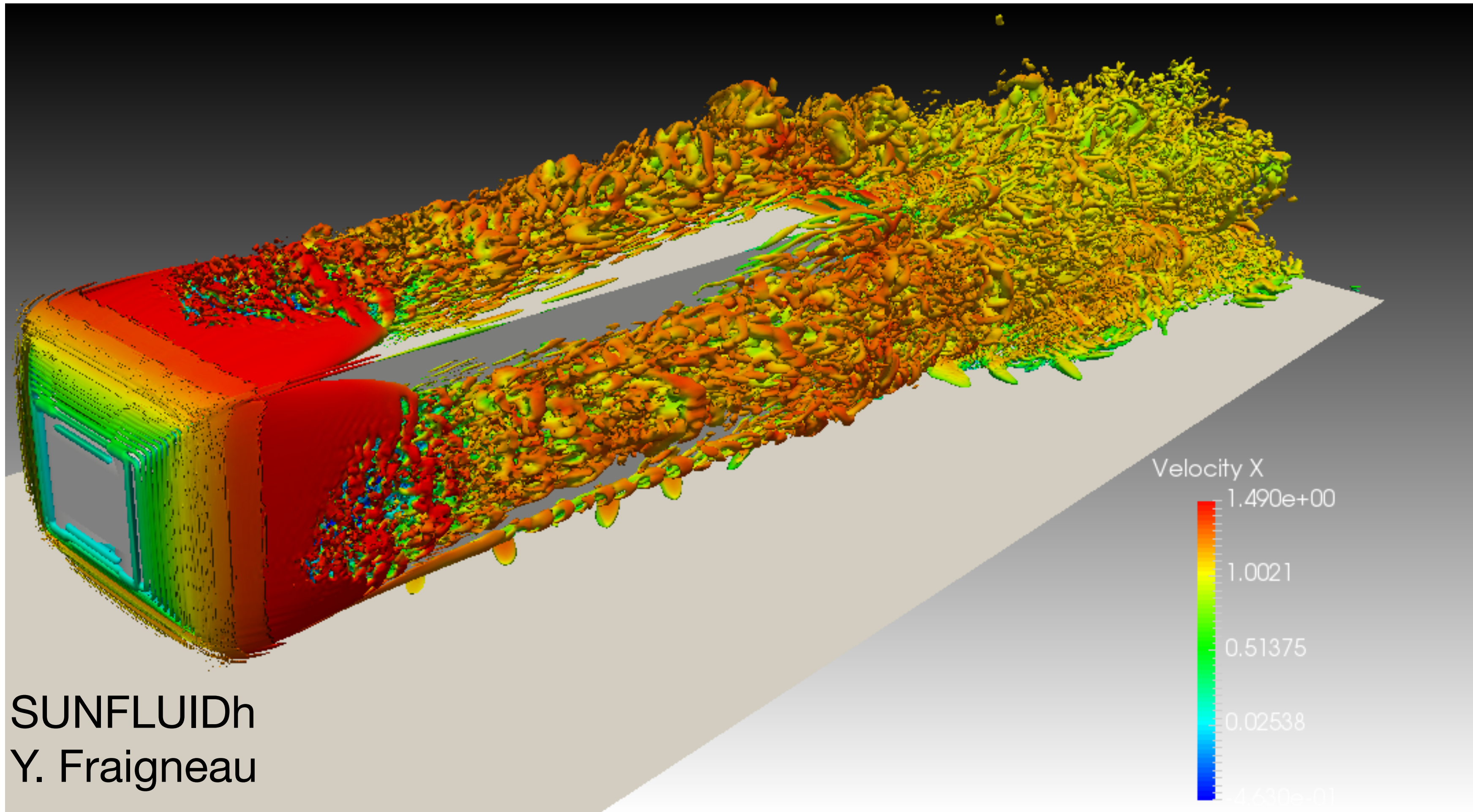


Non-autonomous model



**Correct
spectral
content**

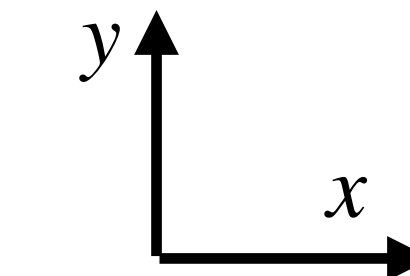
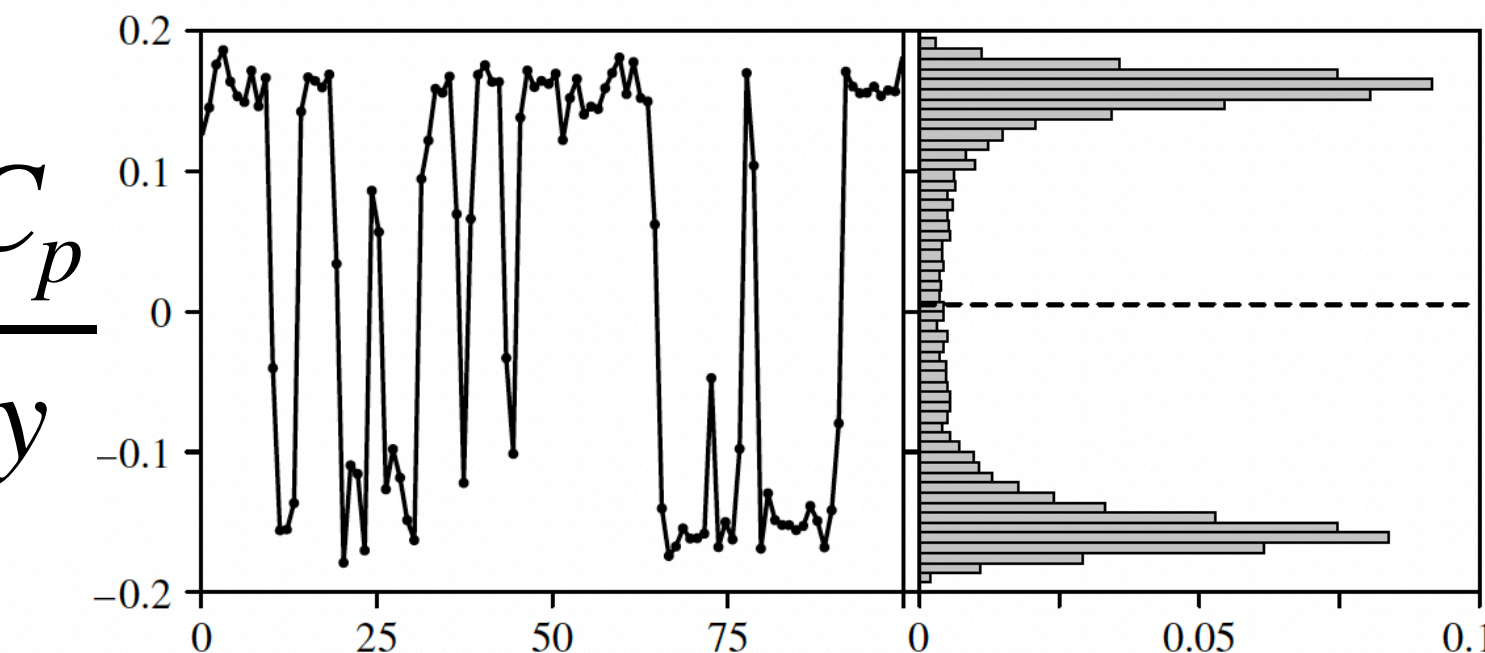
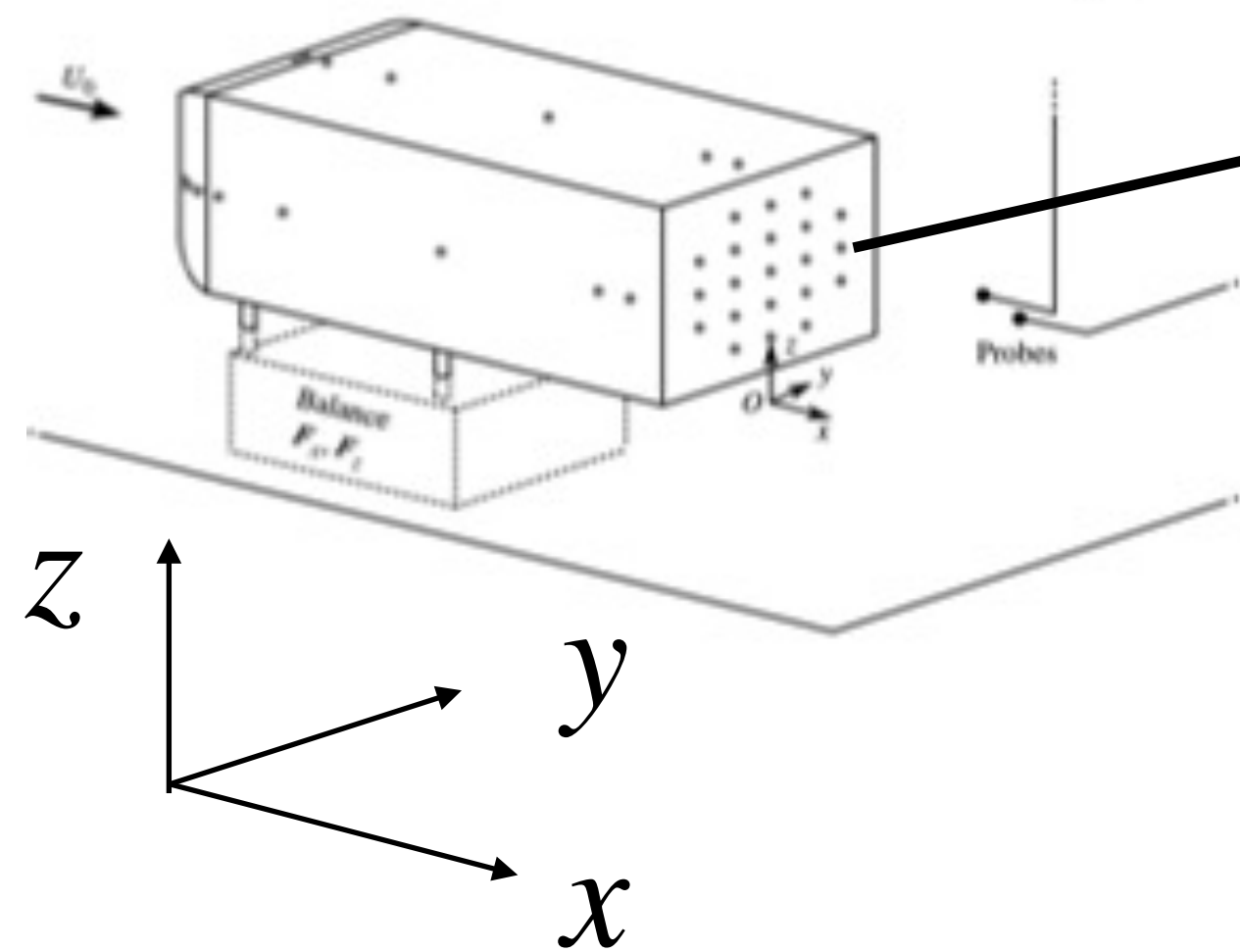
A third example: bluff-body wake



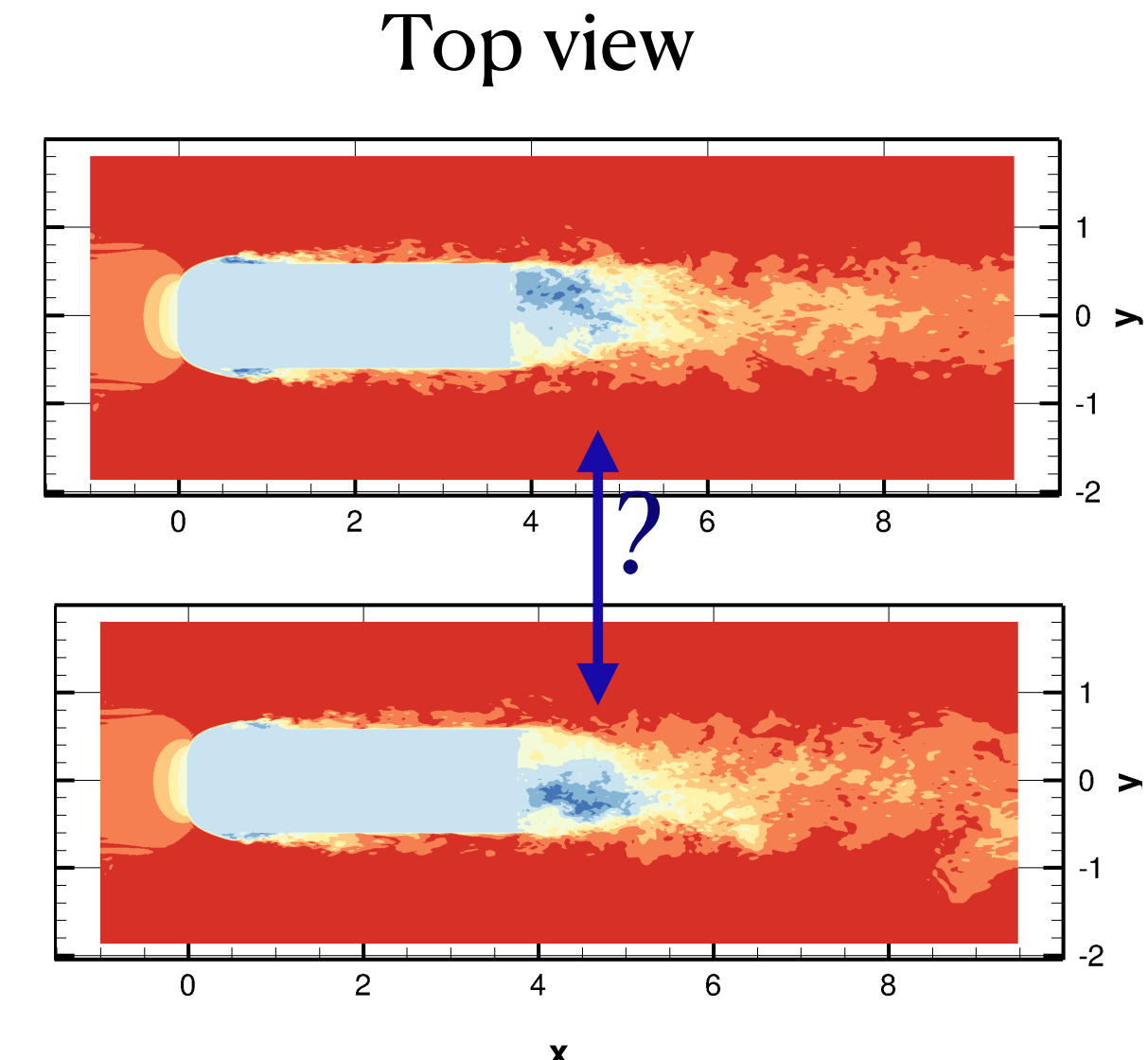
Ahmed body

A wide diversity of time scales

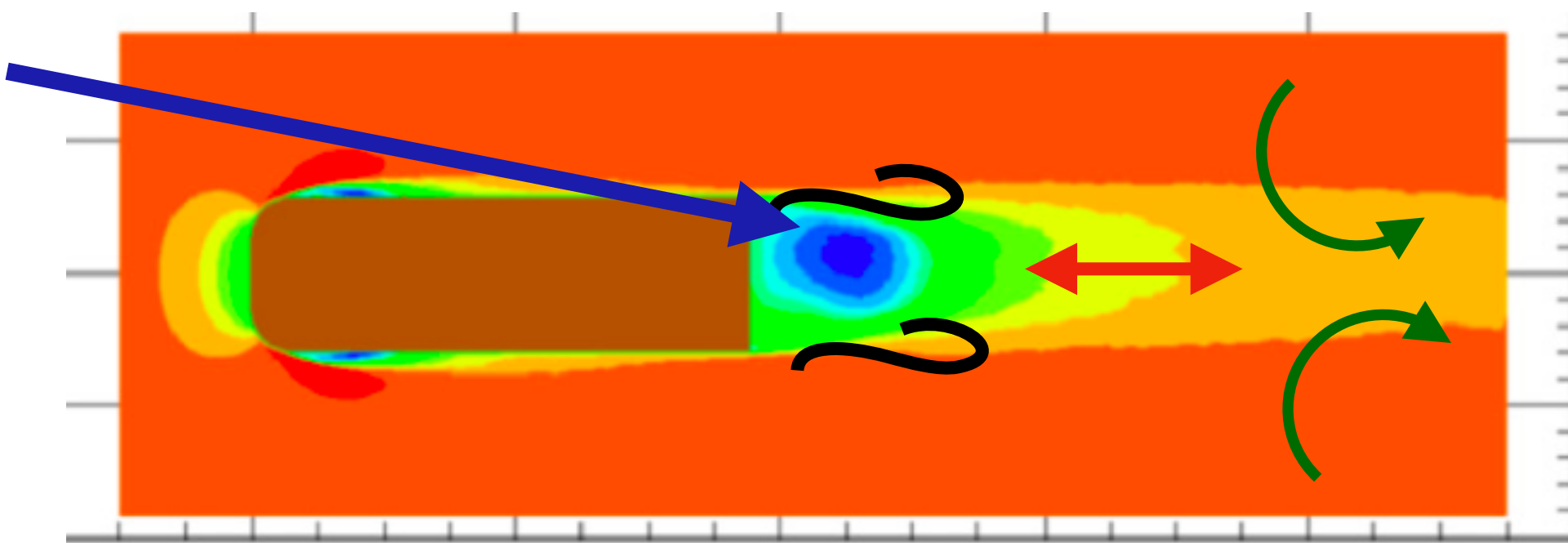
Grandemange and Cadot
JFM 2013



Intermittent switches between quasi-stationary
wake symmetry-breaking states



- Wake deviation switch $tU/H \sim O(1000)$
- Wake pumping. $tU/H \sim O(10-20)$
- Vortex shedding $tU/H \sim O(5)$
- Shear layer instability $tU/H \sim O(1)$



Can we build a model that captures the switches?

POD analysis

$$u(x, t) = \sum_n a_n(t) \phi_n(x)$$

0.2

Decreasing energy λ_n

Deviation

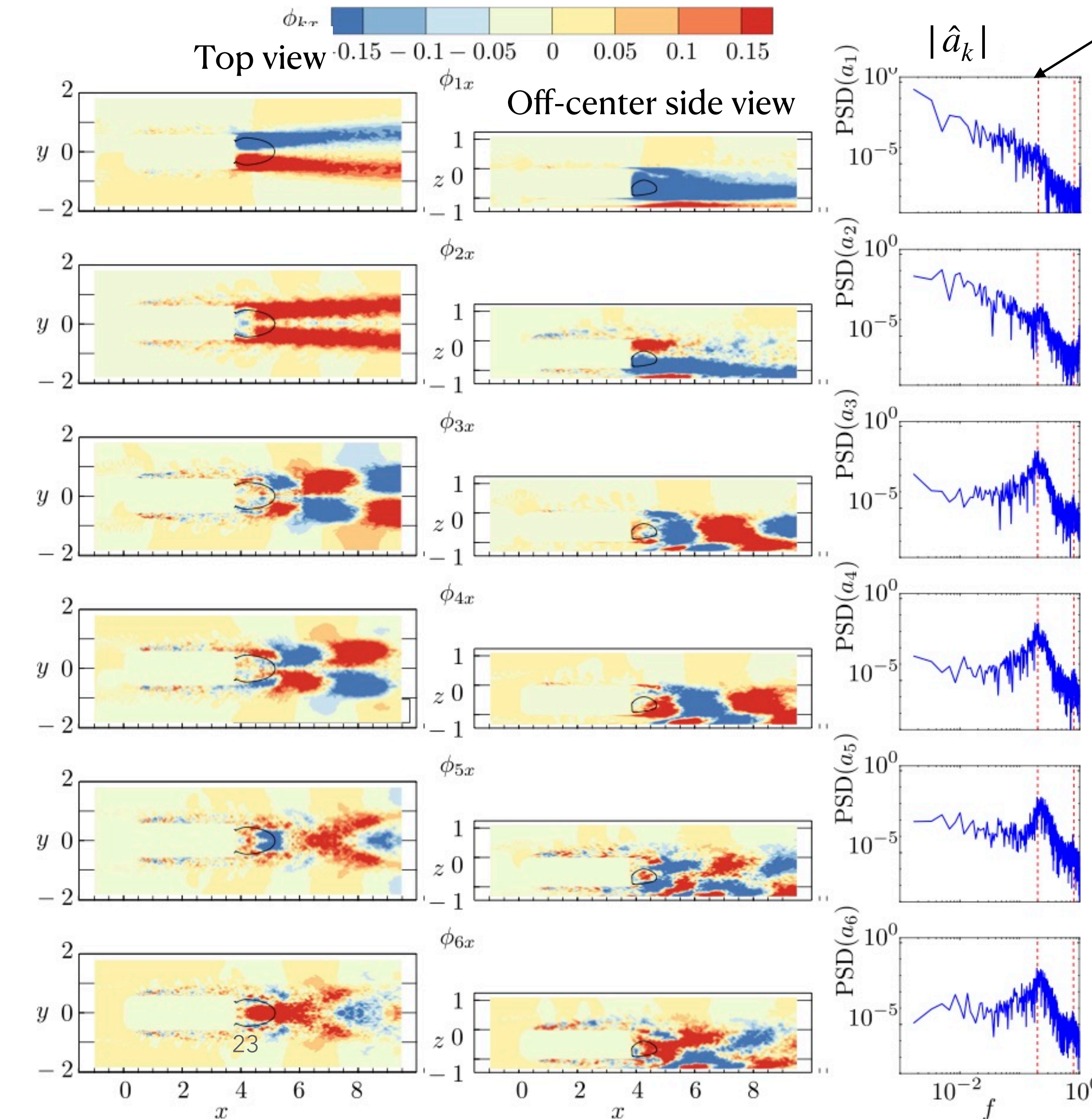
« Switch »

Lateral Shedding

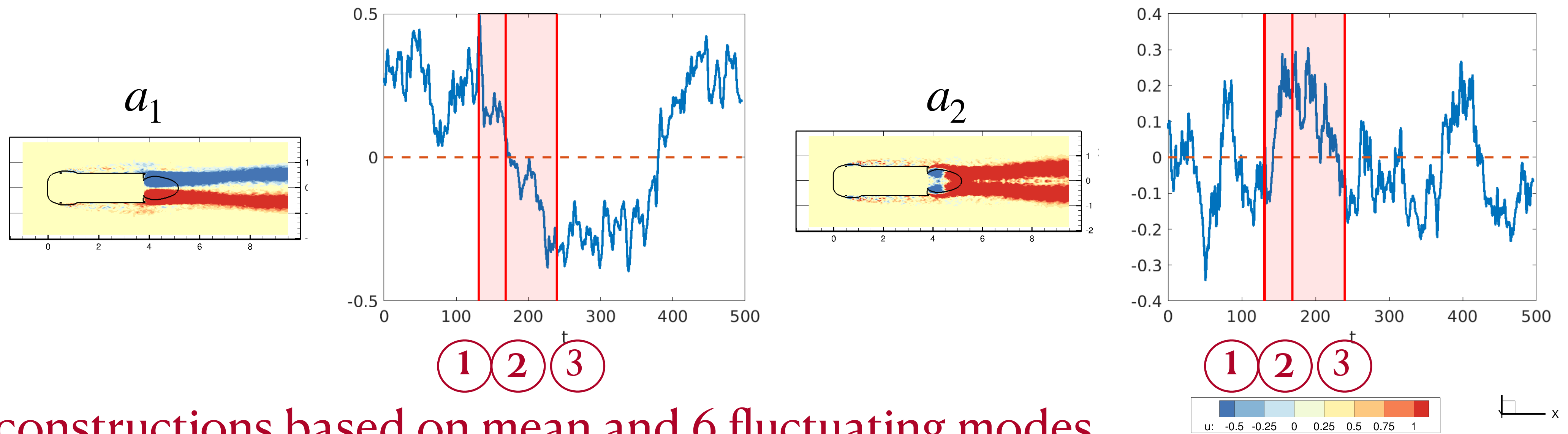
Lateral Shedding

Vertical Shedding

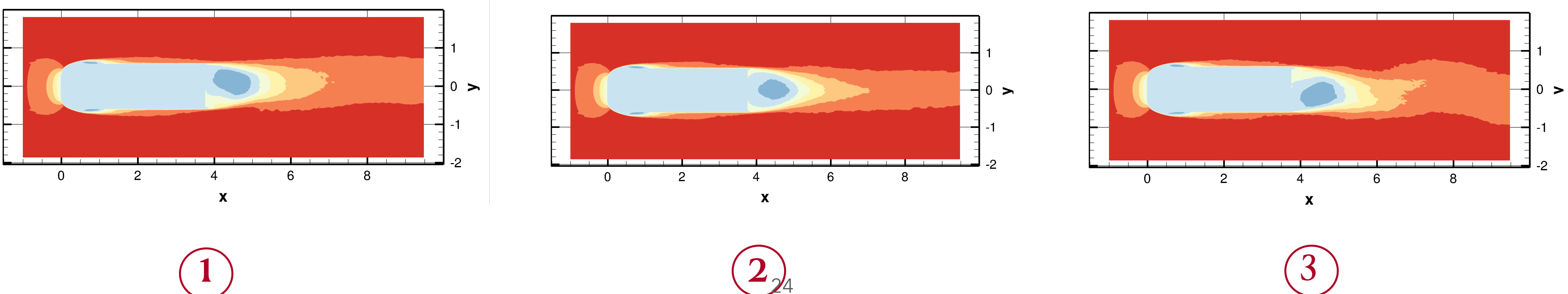
Vertical Shedding



Evolution of the dominant POD modes during a switch



Flow reconstructions based on mean and 6 fluctuating modes



A nonlinear model

$$\dot{a}_0 = 0 \quad (a_0 = 1) \quad \text{Mean}$$

$$\dot{a}_1 = A_1 + 0.011a_1a_2 + 0.019a_0a_3 + 0.023a_0a_4 + 0.045a_3a_5 + 0.005a_1a_6 + \epsilon_1$$

$$\dot{a}_2 = A_2 + 0.12a_0a_5 + 0.11a_0a_6 + 0.007a_2a_3 - 0.018a_1^2 + 0.018a_0^2 + \epsilon_2$$

$$\dot{a}_3 = A_3 + 1.08a_0a_4 - 0.02a_0a_1 + 0.037a_1a_6 - 0.025a_2a_4 - 0.02a_0a_3 + \epsilon_3$$

$$\dot{a}_4 = A_4 - 1.08a_0a_3 - 0.16a_0a_1 - 0.04a_1a_5 + 0.025a_2a_3 - 0.02a_0a_4 + \epsilon_4$$

$$\dot{a}_5 = A_5 + 1.18a_0a_6 - 0.13a_0a_2 + 0.035a_2a_3 - 0.013a_1a_3 + 0.029a_1a_4 - 0.013a_2^2 - 0.02a_0a_5 + \epsilon_5$$

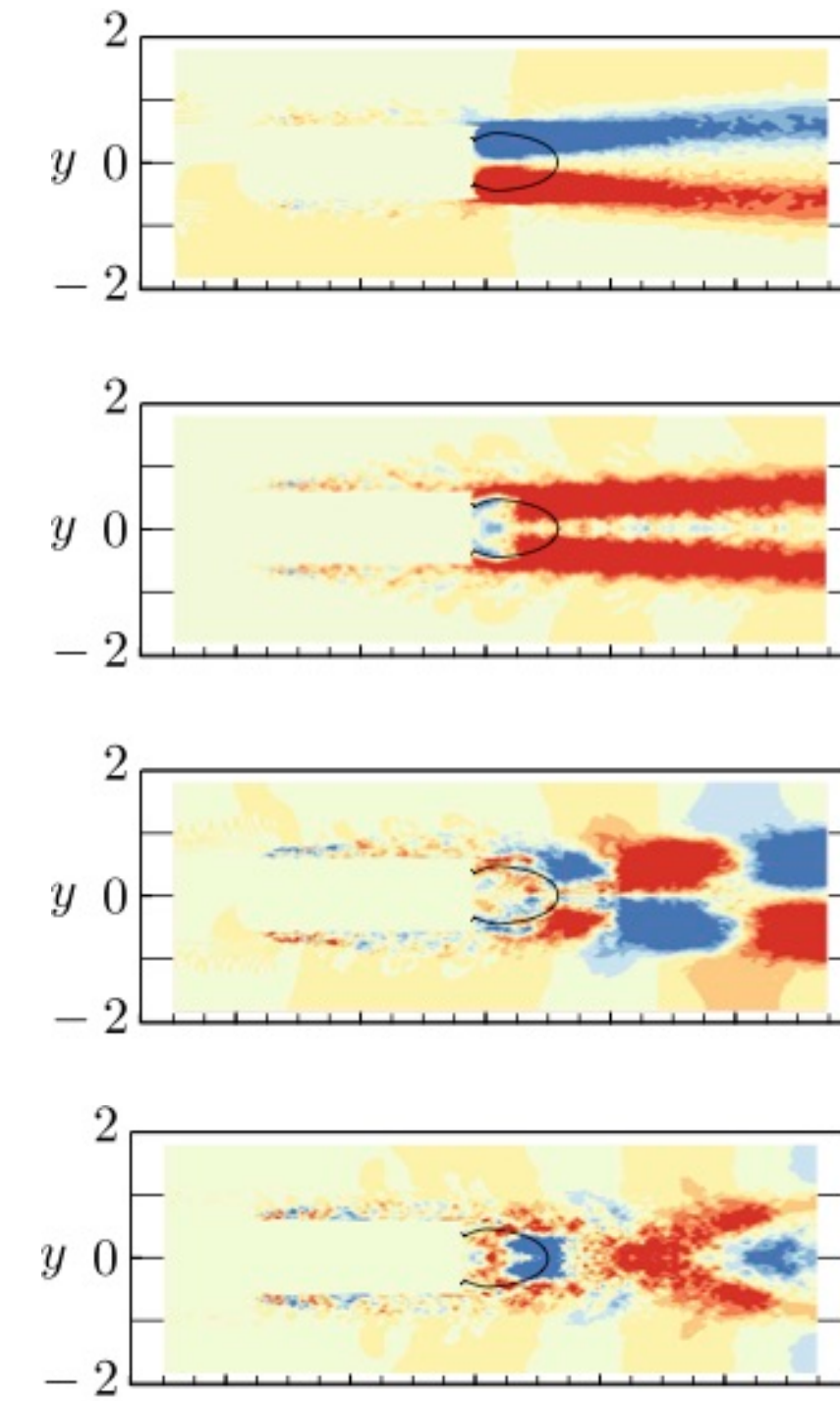
$$\dot{a}_6 = A_6 - 1.18a_0a_5 - 0.26a_0a_2 - 0.026a_2a_5 - 0.02a_1a_3 - 0.02a_0a_6 + \epsilon_6,$$

Von Karman shedding frequencies

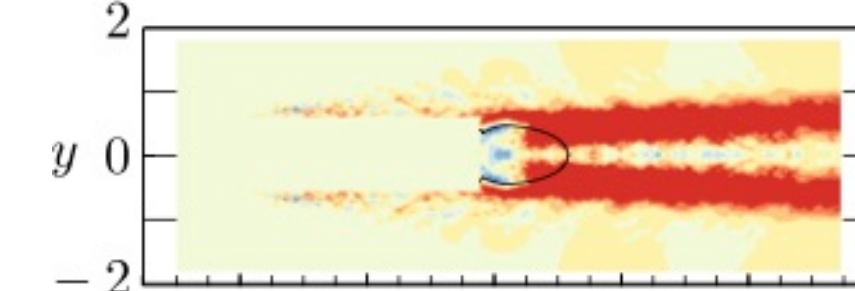
Reflectional symmetry determines form of quadratic terms

Long-time integration of the model

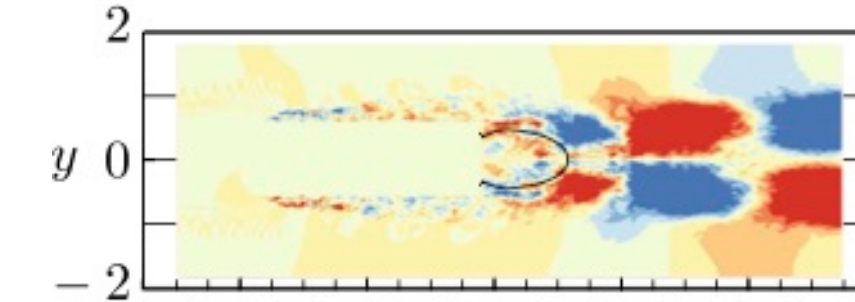
1: Deviation



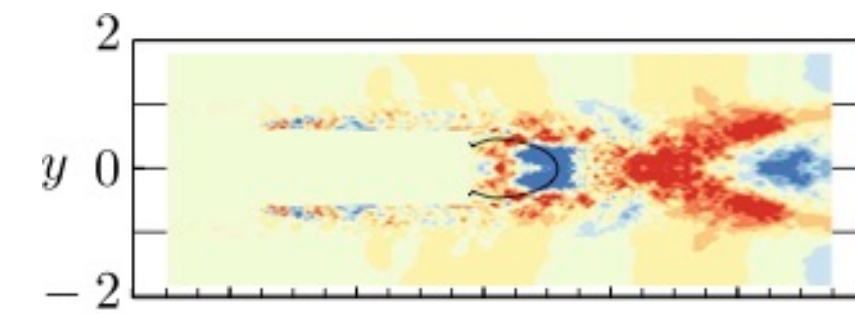
2: Switch



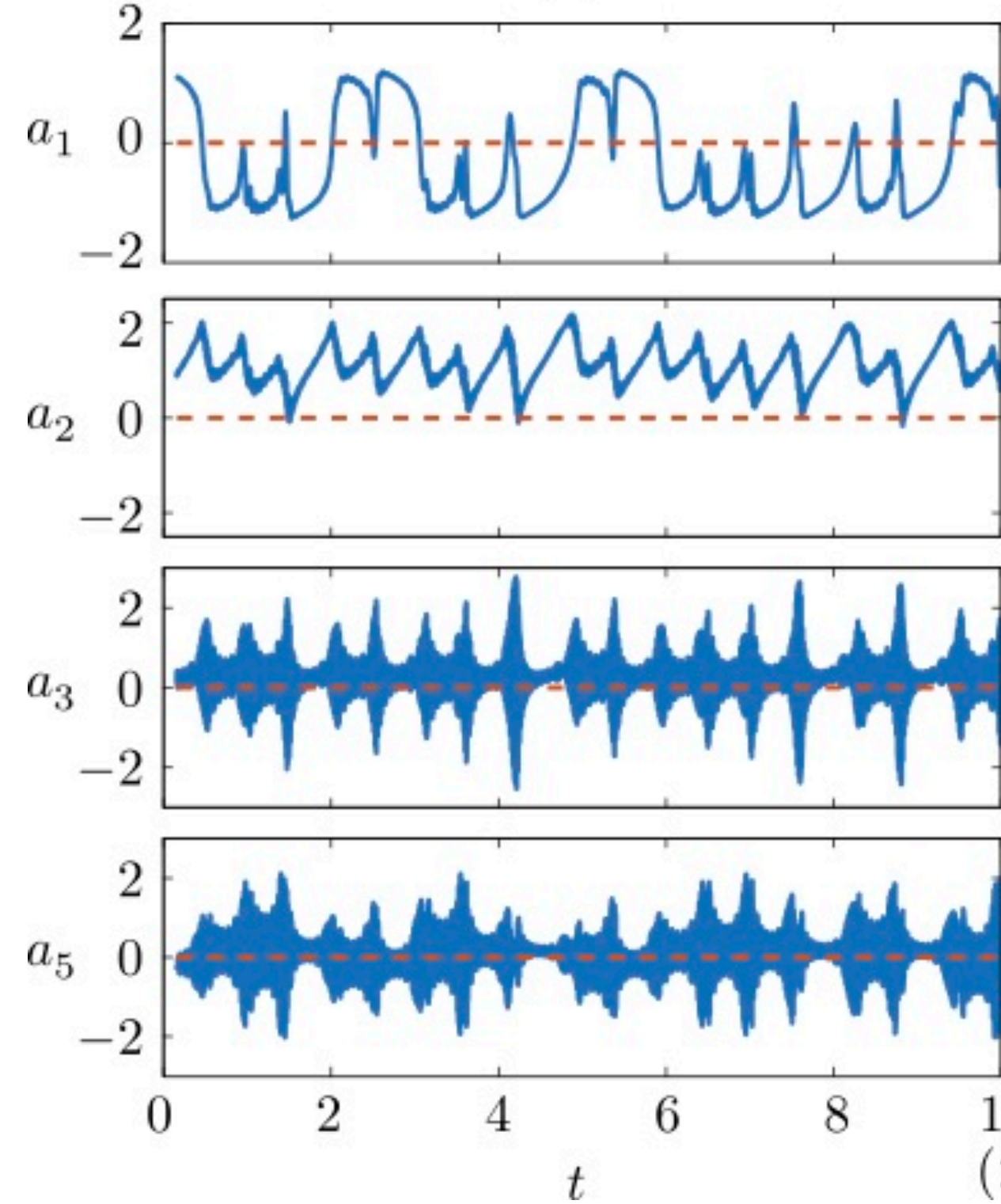
3: Lateral VK



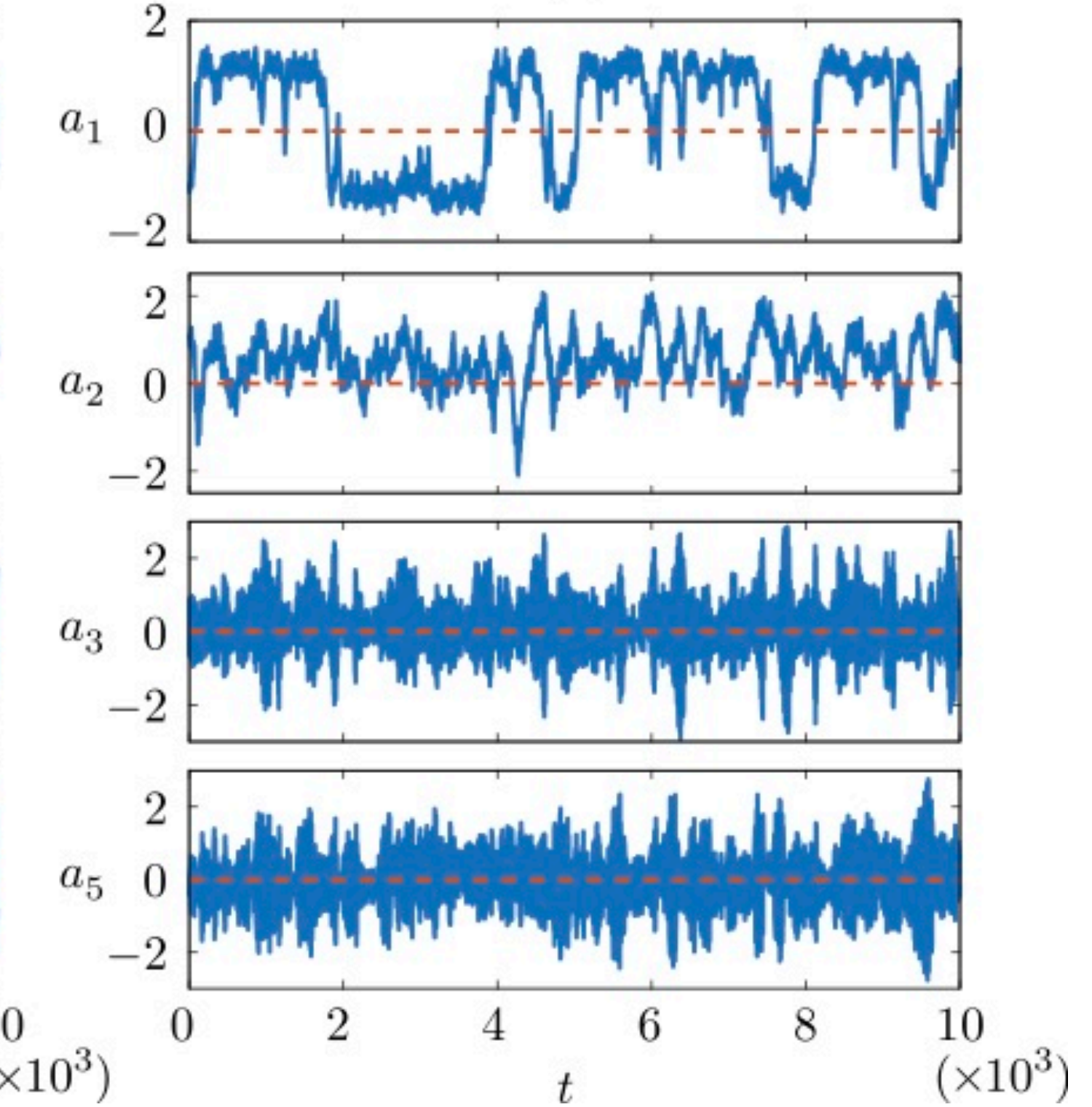
5: Vertical VK



Without noise $\sigma = 0$



With noise $\sigma = 0.07$



Model produces switches that are triggered by excitation of shedding modes.

Addition of noise improves agreement with DNS.

Summary

- POD-based models can capture some key dynamics of complex, high-dimensional separated flows (also convection problems!)
- More work is needed to improve the models
- Machine learning opens new possibilities to better link data and physics
 - improve small-scale modelling
 - handle missing information

References

Low-dimensional analysis and modelling of the flow over a forward-facing step. B. Podvin, **Y. Fraigneau**, Journal of Fluid Mechanics 2024

Low-order modelling of the wake dynamics of an Ahmed body, B. Podvin, **S. Pellerin, Y. Fraigneau, G. Bonnavion, O. Cadot**, Journal of Fluid Mechanics 2021

Low-order models for predicting radiative transfer effects on Rayleigh-Bénard convection in a cubic cell at different Rayleigh numbers, **L. Soucasse, B. Podvin, P. Rivièvre, A. Soufiani**, Journal of Fluid Mechanics 2021

Thank you